Structure of liquid Sn over a wide temperature range from neutron scattering experiments and first-principles MD simulation: A comparison to liquid Pb

Structure of liquid Sn over a wide temperature range from neutron scattering experiments and first-principles molecular dynamics simulation: A comparison to liquid Pb

T. Itami*
Division of Chemistry, Graduate School of Science, Hokkaido University, Sapporo 060-0810, Japan

S. Munejiri,† T. Masaki, and H. Aoki
National Space Development Agency of Japan (NASDA), 2-1-1 Sengen, Tsukuba 305-8505, Japan

Y. Ishii
Advanced Science Research Center, Japan Atomic Energy Research Institute (JAERI) Tokai-Mura, Naka-Gun, Ibaraki 319-1195, Japan

T. Kamiyama
Division of Quantum Energy, Graduate School of Technology, Hokkaido University, Sapporo 060-8628, Japan

Y. Senda,‡ F. Shimojo,§ and K. Hoshino
Faculty of Integrated Arts and Sciences, Hiroshima University, Higashi-Hiroshima 739-8521, Japan
(Received 12 September 2002; published 10 February 2003)

The structure of liquid Sn was studied by neutron scattering experiments in the widest temperature range that was ever performed. Though, on increasing temperature, the existence of the shoulder in the structure factor, $S(Q)$, becomes less clear in the change of the overall shape of the $S(Q)$, the structure related to this shoulder seems to be present even at 1873 K. The first-principle molecular-dynamics (FPMD) simulation was performed for the first time for liquid Sn by using the cell size of 64 particles. The calculated results well reproduced $S(Q)$ obtained by the neutron experiments. The angle distribution, $g^{(3)}(\theta,r_c)$, was evaluated for the angle between vectors from centered atom to other two atoms in spheres of cutoff radii r_c's. The $g^{(3)}(\theta,r_c)$ shows that, with the decrease of r_c from 0.4 to 0.3 nm, a rather sharp peak around 60 ° disappears and only a broad peak around 100 ° remains; the former peak may be derived from the feature of the closely packed structures and the latter one is close to the tetrahedral angle of 109 °. In addition, the coordination number, *n*, of liquid Sn counted within the sphere of $r_c=0.3$ nm is found to be 2–3 and does not change with the increase of temperature even up to 1873 K. These facts indicate that at least the fragment of the tetrahedral unit may be essentially kept even at 1873 K for liquid Sn. For comparison, the FPMD simulation was performed for the first time also for liquid Pb. No sign of the existence of the tetrahedral structure was observed for liquid Pb. Unfortunately, the self-diffusion coefficients, *D*'s, obtained from this FPMD for liquid Sn do not agree with those obtained by the microgravity experiments though the structure factors, $S(Q)$'s, are well reproduced. To remove the limitation of the small cell size of the FPMD, the classical molecular-dynamics simulations with a cell size of 2197 particles were performed by incorporating the present experimental structural information of liquid Sn. Obtained *D*'s are in good agreement with the microgravity data.

DOI: 10.1103/PhysRevB.67.064201 PACS number(s): 61.25.Mv, 61.12.−q, 61.20.Ja

I. INTRODUCTION

The accurate information of the structure of liquids is essential for the exact theoretical analysis of physicochemical properties, such as electron transport properties, atomic transport properties, etc. For example, the well known Ziman theory[1] is very successful in predicting the electron transport properties of simple liquid metals by coupling the structure factor, $S(Q)$, of liquids with pseudopotential of ions. The $S(Q)$ of liquids determines the configuration of ions (scattering centers for electrons) whose electron scattering strength is given by the ''weak'' pseudopotential in the scheme of the Born approximation in the scattering theory. Such a viewpoint is successful also to predict thermodynamic properties.[2]

However, as for atomic transport properties, various theories have been proposed from a point of view of kinetic theory of liquids, Langevin equation for the velocity autocorrelation function (VAF) and the mode coupling theory.[3–6] These theories require $S(Q)$ of liquids as basic input information and many theories, except for the hard sphere model, have not always been successful in reproducing the experimental values[5] particularly for polyvalent liquid metals. This difficulty for the understanding of the atomic transport properties in liquids is derived from the complexity in the many body character in atomic motions in liquids. In the case of hard sphere model, this many body effect is treated in a rather simple manner by the so-called backscattering factor, which can be evaluated by comparing the self-diffusion coefficient given by the Enskog theory[7] to that given by the computer simulation of hard spheres.[8] The hard sphere model itself stresses the importance of the role of the packing of atoms or that of the repulsive part of the inter-atomic potential on the structure of liquids and its validity has been

limited to rather simple liquids near the melting temperature.[5]

In addition to these difficulties in theoretical aspects, there have been additional difficulties on the studies of diffusion, particularly in liquids with high melting temperatures. Such liquids are important for the study of the mechanism of diffusion because of their wide liquid temperature range, in which the temperature dependence of diffusion coefficient can be investigated. Moreover, liquid metals and the melt of semiconductors, which are important also from the applied science, are such liquids with high melting temperatures. However, experiments of diffusion in such liquids on the ground have been spoiled by the presence of the inevitable convection in liquid samples.[9] Because of its absence of convection under microgravity, the International Space Station (ISS), whose construction has already started, is expected to provide the breakthrough for the study of diffusion in liquids. In this respect, the study of the structure of liquids in the wide temperature range is also important for the theoretical analysis of diffusion mechanism in liquids.

The liquid Sn is a good material for the study of the self-diffusion phenomena theoretically because the self-diffusion coefficient itself has been measured under microgravity of space shuttle with no convection in the very wide temperature range, for example, from 543 to 1048 K by Frohberg *et al.*,[9,10] from 902 to 1614 K by Itami *et al.*[11] and 1622 K by Yoda *et al.*[12] To analyze these results, it is important to obtain experimentally the structure factor, $S(Q)$, of liquid Sn in such a wide temperature range.

As for the experimental structure analysis of liquid Sn, Waseda[13] reported the $S(Q)$ of liquid Sn by the x-ray diffraction technique and Takeda *et al.*[14] by the neutron diffraction technique. The temperature range studied in these previous structure studies is rather limited to a lower temperature range compared with that of the study of self-diffusion under microgravity described above.

It is interesting to consider the structure of liquid Sn among the trend of all group IVB(14) elements. There exists a systematic trend in structural and physicochemical properties for solids of group IVB(14) elements.[15] In the case of heaviest Pb, the stable crystal shows a face centered cubic structure and its electronic properties are metallic. The lightest Si has a diamond structure. The next lightest element, Ge, also has a diamond structure. The electronic properties of these Si and Ge crystals are typically semiconductor like. On the other hand, the crystal structure of Sn is intermediate between the heaviest element, Pb, and the lighter elements, Ge and Si. The crystal of Sn has a tetragonal structure (white Sn or β-Sn) above 286.4 K. Below 286.4 K its crystal structure changes from β form to a form of cubic structure (gray tin or α-Sn). The higher temperature form (β-Sn) has a metallic property and the lower temperature form (α-Sn) shows a character of semiconductors.[16] These systematic trends in the crystal structure and in the electronic structure in group IVB(14) are reflected on the structure of liquid states.[13] For example, the structure factor, $S(Q)$, of liquid Pb is rather simple and well reproduced by the hard sphere model[17] (''simple liquids''). On the other hand, in the lighter Ge a distinct shoulder is present in the high wave number side (''high-Q side'') of the first peak of $S(Q)$. The more distinct shoulder can be seen in the structure factor, $S(Q)$, of the lightest Si in the liquid state. The structure of liquid Sn is intermediate between the liquid structure of the heaviest element, Pb, and that of the lighter elements, Ge and Si. The $S(Q)$ of liquid Sn shows only a small shoulder in the high-Q side of the first peak particularly near the melting temperature.

As for the $S(Q)$ of liquid Sn, Orton[18] proposed a model by extending the double hard sphere model for liquid Ge,[19] Sb,[20] Ga,[21] Si and Bi,[22] all of which show the shoulder in $S(Q)$. A similar model also was proposed by Gabathuler and Steeb[23] for the $S(Q)$ of liquid Sn, Ge, and Si. These shoulders were reproduced by the supposition of two kinds (different diameters) of single component hard sphere structure factor.[17] Petkov and Yunchov[24] applied the reverse Monte Carlo method for the analysis of the structure of liquid Sn, Ge, and Si near the melting temperature. The obtained atomic arrangement, which reproduces the experimental structure factor of liquid Sn, shows a feature of distorted β-Sn structure though its tendency is weaker than the cases of liquid Ge and Si.

It is also important to consider these models or analyses from a more fundamental point of view. Hereafter, for a while, a review is given for the theoretical interpretation of shoulders in $S(Q)$ mainly for liquid Sn and, if important, for other liquid metals with such shoulders. Silbert and Young[25] proposed the possibility that the origin of the shoulders in $S(Q)$ of liquid Bi may be related to its ledge type interionic potential (''ledge'' in the repulsive type). The correspondence of the double hard sphere model to this ledge type potential was discussed by Orton[18,22] for liquid Sn and liquid Bi. Grimson and Silbert[26] systematically investigated the effect of ledge in the interionic potential on the $S(Q)$ of polyvalent liquid metals by applying a perturbation theory of liquids, in which a hard sphere potential and a ledge potential were taken as the ''reference potential'' and the ''perturbation potential,'' respectively. They found that the square type ledge was better than the Yukawa type one to reproduce the shoulder in $S(Q)$ of liquid Sn. Thus, the ''ledge'' in the interionic potential seems to be important for the appearance of the shoulders in $S(Q)$. Investigations were performed for the systematic trends in the interionic potentials themselves by Heine and Weaire,[27] Hafner and Heine,[28] Yokoyama and Ono,[29] and Hoshino *et al.*[30]

Hafner and Kahl[31] found that this ledge type interionic potential (or interionic potential with a ''wiggle'' in the repulsive part) can be derived from the pseudo-potential theory for various liquid metals and they succeeded in reproducing theoretically the shoulders in the $S(Q)$ of Ga, Ge, and Si based on the refined theory of liquids, that is optimized random phase approximation theory. Shoulders in the $S(Q)$ and the ledge type potential seem to appear because of the interplay between the hard core distance and the wavelength of the Friedel oscillation. Unfortunately, no analysis was performed for the shoulder of $S(Q)$ in liquid Sn. Jank and Hafner[32] presented a systematic analysis of the atomic and electronic structure of liquid group IVB(14) elements by using a classical molecular dynamics (MD) simulation for

atomic structures and a self-consistent linear muffin tin orbital-supercell method for electronic structures. Detailed analyses were given for liquid Si and Ge. Unfortunately, the atomic structure of liquid Sn was not so much analyzed. On the other hand, Mon *et al.*[33] derived the effective interionic potential with a secondary minimum at a small separation by considering the role of the dynamically screened fluctuating dipole–dipole interactions between ion cores (van der Waals interaction). They succeeded in reproducing the shoulders in the $S(Q)$ of liquid Ga by the Monte Carlo computer simulation, in which this newly determined interionic potential with a subsidiary minimum was applied. As for the $S(Q)$ of liquid Ge, Ashcroft[34] discussed the role of the existence of two possible extreme dynamic entities in liquids, atoms with polarizable ion cores, and cluster units (tetrahedral units) with translational, orientational, and vibrational motions. The relation was stressed between the possibility of the existence of cluster units in liquids and the dimer unit or polymerization in the gas phase. Recently, González *et al.*[35] derived the effective interionic potential with the shoulder at the short distance by taking into account the induced core polarization effect. The $S(Q)$ of liquid Ga was calculated with the combination of this effective pair potential and the integral equation of liquids.

The structure of liquids may be sensitive to the temperature variation. Therefore, it is deeply desired to study experimentally the structure of liquid Sn in the extremely wide temperature range and to analyze the obtained information of structures in detail. In addition, the microscopic feature of the structure for liquid Sn must be analyzed freely from these models described above. This is required to confirm the meaning and the validity of these models and to obtain further insight for the understanding of the structure of liquid Sn. For these purposes, the rapidly advancing computer simulations are expected. Unfortunately, up-to-date, classical molecular dynamics (MD) simulations for liquid Sn, based on the Newtonian law of motion, have not been published so much and the microscopic structure of liquid Sn has not yet been analyzed in detail. This may be derived from the fact that, for liquids such as liquid Sn, it is not always easy to find an appropriate effective interionic pair potential, which is needed for the accurate classical MD simulation. Apart from the effective interionic potentials based on the microscopic basis of pseudopotential theories, the many body interatomic potentials have been empirically proposed[36,37] for Ge and Si and are applied to the molecular dynamics for liquid states of Si and Ge.[38–40] The reliability of these many body interionic potentials in liquid states seems to be not as rigorous as that in solid states.[41]

Here, we note the first-principle molecular dynamics (FPMD) simulations,[42] based on the density functional theory in quantum mechanics in which no information about interatomic potential is required for this quantum mechanical technique. To date, for liquid Sn, a preliminary result of FPMD has only been presented by Munejiri *et al.*[43]

The purpose of this paper is to report the structure analyses of liquid Sn in the extremely wide temperature range in terms of neutron scattering experiments and the FPMD simulation. This paper is composed of five sections. Sections II and III describe, respectively, the method of neutron diffraction experiments and that of the FPMD simulation. In Sec. IV the results and detailed discussions are given for the structural analysis of liquid Sn due to both the neutron diffraction and the FPMD simulation. The microscopic feature of the structure of liquid Sn in the wide temperature range is discussed from the static structure factor, $S(Q)$, the radial distribution function, $g(r)$, the angle distribution function in the atomic triplet, $g^{(3)}(\theta, r_c)$, and the distributions of coordination number, $p(n)$. For comparison, results for $g^{(3)}(\theta, r_c)$ and $p(n)$ of liquid Pb are also given from the FPMD simulation. Finally dynamics of atomic motions in liquid Sn are discussed with particular attention to the self-diffusion coefficient obtained under microgravity. A summary is provided in Sec. V.

II. NEUTRON SCATTERING EXPERIMENTS

In order to obtain the $S(Q)$ of liquid Sn, neutron scattering experiments were performed with the use of the triple axes spectrometer (TAS-1) of Japan Research Reactor No.3 (JRR-3M) in Japan Atomic Energy Research Institute (JAERI). The temperatures measured were 573, 773, 1073, 1373, 1673, and 1873 K. The experiments below 1073 K were performed with the use of fused silica cells. Glassy carbon cells were adopted for experiments above 1373 K. The Sn samples with a purity of 99.9999% were melted and purified by removing a small amount of oxide layer carefully. Then, the purified sample was poured into a cylindrical fused silica cell or glassy carbon one. The size of fused silica cell was 8.0 mm inner diameter, 8.6 mm outer diameter, and 30 mm height. That of the glassy carbon cell was 10 mm inner diameter, 10.6 mm outer diameter, and 30 mm height. All procedures for the sample preparation were performed in an Ar gas circulating glove box. Experiments above 1373 K were performed with the use of the ''1800 Celsius High Temperature Furnace'' (prepared by AS Scientific Products) with Nb heating elements. A furnace with nickel-chrome heating elements was employed for experiments below 1073 K. The incident neutron wavelengths, λ's, were 0.085, 0.095, and 0.224 nm, giving a range of scattering wave number, Q ($=4\pi \sin\theta/\lambda$; 2θ: scattering angle), of 5 to 105 nm^{-1}. The scattered intensity was measured with the interval of 0.5 and 1 nm^{-1}, respectively for $Q<60\ \mathrm{nm}^{-1}$ and for $Q>60\ \mathrm{nm}^{-1}$. The counting time of scattered neutrons was typically 8–12 h. Neutron scattering intensities were converted into the structure factor, $S(Q)$, by using standard procedures, which includes subtraction of cell intensities, corrections for absorption,[44] multiple scattering effect,[45] and inelastic effect.[46]

III. THE FIRST-PRINCIPLE MOLECULAR DYNAMICS

The first-principle molecular dynamics (FPMD) simulation was performed for liquid Sn based on the density functional theory with the local density approximation.[47] For the interaction between the valence electrons and the ion, we employed the norm-conserving pseudopotential of Troullier and Martines,[48] which is derived from the calculation of the

atomic electron configuration $5s^2 5p^2 5d^0$. The electronic wave functions were expanded in terms of a plane wave basis set with a cutoff energy of 11 Ryd. The Γ point was used to sample the Brillouin zone of the supercell. The Γ-point sampling saves computing time and prevails in the study of liquid metals, though incorporation of the details of band structural information may also be important. The Kohn-Sham energy functional was minimized by the preconditioned conjugate-gradient method.[49–51] Then, the forces on the ions were calculated using the Hellmann-Feynman theorem. The MD simulations were carried out with 64 atoms in a cubic supercell from 773 to 1873 K. For the density of the system, experimental values[52] were used. Corresponding to this temperature range, the mass and the number densities of the system were, respectively, 6.82×10^3–6.15×10^3 kg m^{-3} and 34.6–31.2 nm^{-3}; the lengths of the side of the cubic supercells were 1.23–1.27 nm. The constant temperature simulations were performed using the Nosé-Hoover thermostat[53,54] for 10 000 steps with a time step of 3.6–4.8 fs. The initial atomic configurations were generated by a classical MD simulation with the effective pair potential calculated from the experimental structure factor.[13] The FPMD was performed using the supercomputer Fujitsu VPP500 at the Center for Promotion of Computational Science and Engineering (CCSE) of JAERI and the workstations composed of the Alpha 21264, which was installed at the National Space Development Agency of Japan (NASDA).

The FPMD was performed also for liquid Pb in order to compare in detail the microscopic structure of liquid Sn with that of liquid Pb, which is a typical simple liquid metal belonging to same group IVB(14) elements. The method of simulation was essentially similar to that of liquid Sn. The different parts from the case of liquid Sn were described below. The norm-convergent pseudopotential was constructed from the calculation of the atomic electron configuration $6s^2 6p^2 6d^0$. The electronic wave functions were expanded in terms of a plane wave basis set with a cutoff energy of 10 Ryd. The MD simulations were carried out with 100 atoms in a cubic supercell at 613 and 1623 K. The density employed for simulation was derived from the experimental values,[55] 10.6496×10^3 kg m^{-3} for 613 K and 9.264×10^3 kg m^{-3} for 1823 K. The constant temperature simulations were performed for 3000 steps with a time step of 3.6 fs. The initial atomic configuration adopted was a random distribution of 100 atoms on the grid, which was constructed by dividing the supercell into $5\times5\times5$ square segments.

IV. RESULTS AND DISCUSSION

A. The static structure of liquid Sn from neutron scattering experiments

In the present experiments, the adoption of the glassy carbon cell enabled us to perform neutron diffraction experiments of liquid Sn above 1373 K. Figure 1 shows a typical example of the scattering profiles at 1673 K both for empty cell only and that of liquid Sn contained in the glassy carbon cell. On the elimination of the contribution of sample cell, the glassy carbon cell was found to be easier than cells made of crystalline materials because of no Bragg's peak, as shown in Fig. 1.

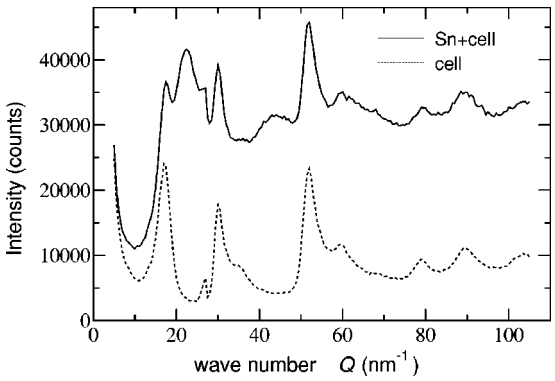

FIG. 1. The typical example of the scattered neutron intensities at 1673 K using the glassy carbon cell; solid line: the scattered intensity due to liquid Sn contained in the glassy carbon cell; dotted line: that due to the glassy carbon cell only.

In Fig. 2, the structure factors, $S(Q)$'s, of liquid Sn obtained are shown as a function of wave number, Q. Experimental error bars of the measured $S(Q)$ are estimated to be 0.5% from the count number of neutrons in the Q range up to 105 nm^{-1}. The error bars of $g(r)$ from the Fourie transform of measured $S(Q)$ depend mainly on those of this measured $S(Q)$. In the case of measurement at 1373 K, some slight additional errors may be included in the Q range from 85 to 105 nm^{-1}. The cause of this exceptional error at 1373 K above 85 nm^{-1} is not known to authors though there is a possibility that some problem was present for the preparation of this new material cell used and a slightly short accumulation time at this temperature. The obtained $S(Q)$ in the present study is in good agreement with previous data[13,14] at corresponding temperatures except for slightly larger value in the low Q region. The value in this low Q region does not affect the evaluation of the radial distribution function, $g(r)$,

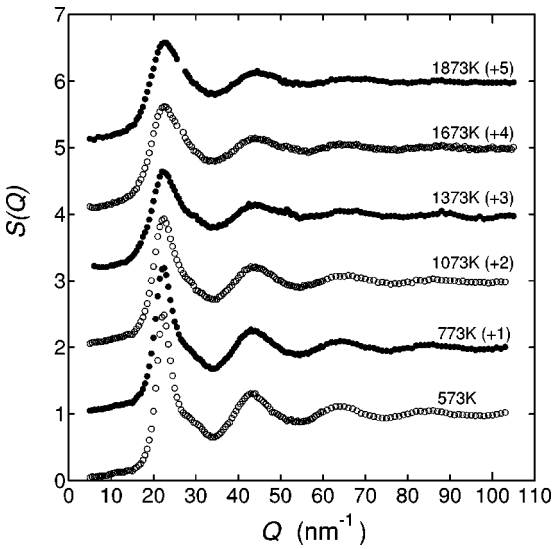

FIG. 2. The structure factor, $S(Q)$, as a function of wave number, Q, of liquid Sn, obtained in the present experiment.

TABLE I. The characteristic parameters of structure factor, $S(Q)$, of liquid Sn; $S(Q_1)$ and Q_1 indicate the first peak value of $S(Q)$ and the corresponding Q value; $S(Q_2)$ and Q_2 indicate the second peak value of $S(Q)$ and the corresponding Q value.

T (K)	Q_1 (nm^{-1})	$S(Q_1)$	Q_2 (nm^{-1})	$S(Q_2)$	Q_2/Q_1	$S(Q_2)/S(Q_1)$
573	22.34	2.498	43.08	1.309	1.93	0.524
773	22.32	2.198	43.03	1.269	1.93	0.577
1073	22.38	1.936	43.10	1.215	1.93	0.628
1373	22.20	1.649	43.99	1.149	1.98	0.697
1673	22.66	1.616	44.00	1.144	1.94	0.708
1873	22.70	1.581	44.50	1.153	1.96	0.729

though there still remains an unknown scattering effect to be removed. The structure parameters characteristic to the present $S(Q)$'s are shown in Table I. At low temperatures, the $S(Q)$ shows shoulders clearly around $Q=28$ nm^{-1}, which is situated in the high-Q side of the first peak of $S(Q)$. With increasing temperature, the first peak of $S(Q)$ becomes lower and broader and, at a first look, the shoulder seems to disappear at higher temperatures. However, it is to be noted that the values of $S(Q)$ around this shoulder remain to be rather constant with the increase of the temperature and the shape of the first peak of $S(Q)$ remains to be asymmetrical even at the highest temperature, 1873 K.

Here it is important to refer to the criterion of the classification of the structure of liquid metals due to Waseda.[13] According to this criterion the structure of liquid metals can be classified into three categories, ''categories I, II, and III.'' The liquid structure of ''category I'' (such as liquid Al and Pb) is characterized by the symmetrical first peak of $S(Q)$ and also by the fact that the ratio Q_2/Q_1 is 1.86 where Q_1 and Q_2 are, respectively, the wave number, Q, of the first peak of $S(Q)$ and that of the second peak of $S(Q)$. Waseda[13] showed that the structure of this ''category I'' can be well reproduced by the hard sphere structure factor.[17] In addition, this ratio, 1.86, remains to be unchanged even at a low packing fraction, η, or at a high temperature. Therefore, the liquid structure of ''category I'' is considered to be rather simple. The asymmetrical first peak is observed for the $S(Q)$ of ''category II'' liquid metals such as liquid Zn. A shoulder is observed in the high-Q side of the first peak of the $S(Q)$ for ''category III'' liquid metals. Liquid Sn can be classified into this ''category III.'' The ratio Q_2/Q_1 of both ''categories II and III'' differs considerably from 1.86. Unfortunately, to date, the temperature dependence of this ratio has not yet been discussed in detail for ''categories II and III.'' Therefore, the temperature dependence of this ratio, Q_2/Q_1, was investigated in detail for liquid Sn in the wide temperature range studied here. Figure 3 indicates that the slightly anomalous (larger) value of this ratio was obtained at 1373 K. This may come from slightly poor reliability of experimental $S(Q)$ at 1373 K compared with the $S(Q)$'s at other experimental temperatures, as described above. Anyway, the ratio Q_2/Q_1 for liquid Sn deviates largely from 1.86, particularly in the high temperature range. For comparison, this ratio was evaluated also for liquid Pb, which is a typical ''category I'' liquid metal. The evaluation of this ratio for liquid Pb was performed based on the $S(Q)$'s in the Table App.8-6 of Waseda.[13] This ratio is found to remain close to 1.86 even at higher temperatures than the melting temperature, as can be seen in Fig. 3. This indicates that the deviation from the simple liquid metals is significant for liquid Sn even at a high temperature, 1873 K.

Figure 4 shows the radial distribution functions, $g(r)$'s, which were obtained from experimental $S(Q)$'s by the Fourier transform. The upper limit of this Fourier transform was taken to be 105 nm^{-1} for $S(Q)$'s at all experimental tem-

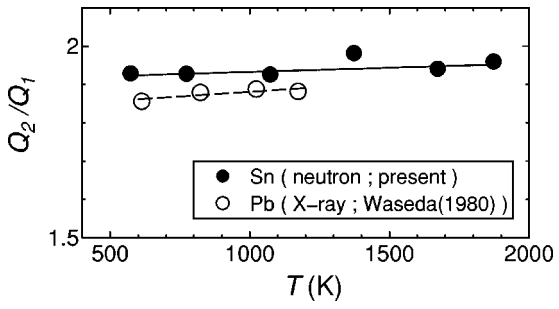

FIG. 3. The temperature dependence of the ratio between Q_1 and Q_2; Q_1 indicates the wave vector of the first peak of $S(Q)$ and Q_2 indicates that of the second peak.

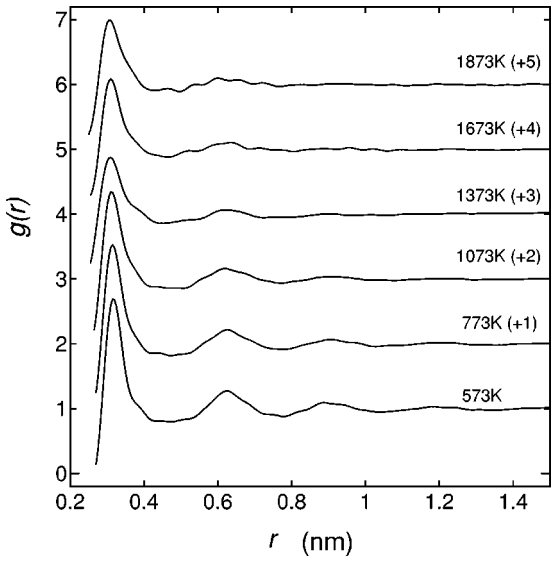

FIG. 4. The radial distribution function, $g(r)$, obtained in the present experiment.

TABLE II. The characteristic parameters of radial distribution function, $g(r)$, of liquid Sn; $g(r_1)$ and r_1 indicate the first peak value of $g(r)$ and the corresponding r value; $g(r_2)$ and r_2 indicate the second peak value of $g(r)$ and the corresponding r value.

T (K)	r_1 (nm)	$g(r_1)$	r_2 (nm)	$g(r_2)$	r_2/r_1	$g(r_2)/g(r_1)$	The first coordination number
573	0.3169	2.697	0.6241	1.274	1.97	0.472	10.7
773	0.3149	2.527	0.6253	1.217	1.99	0.482	10.2
1073	0.3121	2.347	0.6188	1.162	1.98	0.495	9.6
1373	0.3089	1.877	0.6203	1.066	2.01	0.568	8.6
1673	0.3099	2.086	0.6354	1.104	2.05	0.529	8.6
1873	0.3069	1.998	0.6007	1.099	1.96	0.550	8.3

peratures except for 1373 K. It was taken to be 85 nm^{-1} in the case of 1373 K. The effect of this upper cutoff in Q appeared as the irregular behavior in the low r region. Therefore, the $g(r)$ in this region was omitted in Fig. 4. The $g(r)$ in this low r region does not affect the evaluated first coordination number. The characteristic parameters of these $g(r)$'s are given in Table II, in which the first coordination numbers are also shown. The first coordination numbers, which represent the numbers of atoms around the first peak of $g(r)$, were calculated from the conventional method,[13] that is the first peak area of $4\pi r^2 g(r)$ up to the first minimum. The first coordination number at 1373 K is slightly small due to the insufficient accuracy of $S(Q)$ at this temperature as described above. The height of the first peak in $g(r)$ becomes lower with the increase of the temperature for liquid Sn, as is the case of many other liquid metals. The characteristic feature of the $g(r)$ for liquid Sn is seen between the first peak position (r_1) and the second one (r_2). The $g(r)$ of liquid Sn in this region is larger and shows ''flat shape'' or only ''slight minimum.'' This behavior is quite different from the ''clear minimum'' for ''category I'' liquid metals, such as liquid Pb. This peculiar behavior of $g(r)$ for liquid Sn can be seen also in the Table App.8.17 in Waseda.[13] The typical values are, for example, 0.8–0.9 for a ''flat shape value'' of liquid Sn and 0.6–0.7 for a ''clear minima'' value of liquid Pb. Figure 4 shows that this ''flat shape'' tendency for liquid Sn can be seen even at higher temperatures. In spite of such anomalous behaviors in $g(r)$ for liquid Sn, the first coordination number of liquid Sn decreases monotonously from 10.7 to 8.3 with the increase of temperature from 573 to 1873 K, as explicitly shown in Table II. For comparison, the first coordination number was evaluated also for liquid Pb, which is a typical ''category I'' liquid metal, based on the $g(r)$'s in Table App.8.17 due to Waseda.[13] From the temperature dependence of the first coordination number, no particular difference can be found between liquid Sn and liquid Pb, as shown in Fig. 5.

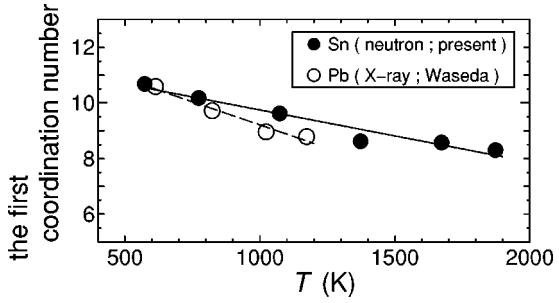

FIG. 5. The temperature dependence of the first coordination number of liquid Sn and liquid Pb (Ref. 13).

B. Microscopic structures of liquid Sn from the FPMD simulation

The molecular-dynamics simulation is important to extract the microscopic information of liquid structures, which is not always obtainable from the scattering experiments of liquids. Therefore, in this study, the FPMD simulation of liquid Sn was performed in addition to the neutron scattering experiment. At first, in Figs. 6 and 7, the structure factors, $S(Q)$'s, and the radial distribution functions, $g(r)$'s, were compared, respectively, with those obtained by the FPMD simulation. The results of FPMD simulation are in good agreement with those of neutron scattering experiments. The

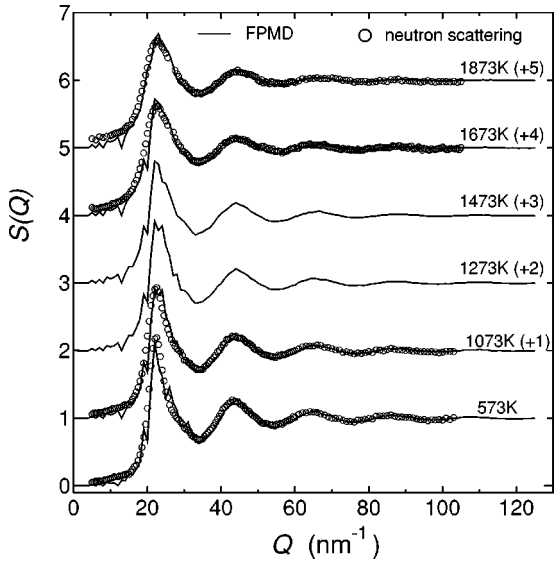

FIG. 6. The comparison of the structure factor, $S(Q)$, of liquid Sn between the present experiment (open circle) and the first-principle molecular-dynamics (FPMD) simulation (solid line).

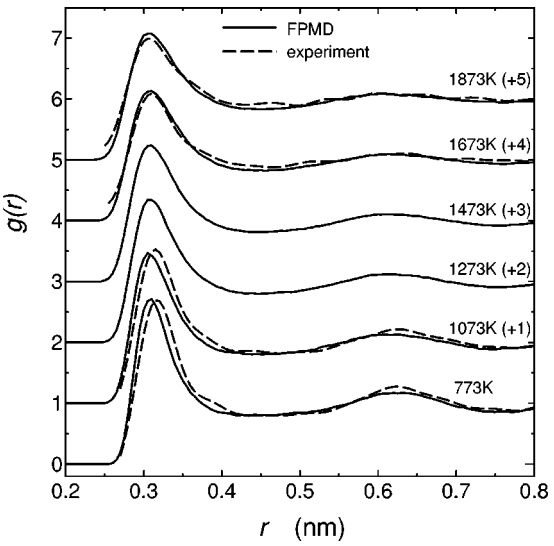

FIG. 7. Comparison of the radial distribution function, $g(r)$, of liquid Sn between the present experiment (open circle) and the first-principle molecular-dynamics (FPMD) simulation (solid line).

shoulder in the experimental $S(Q)$ was reproduced clearly in the high-Q side of the first peak, around $Q=28$ nm^{-1} particularly at low temperatures. In addition, the characteristic feature of $g(r)$, large value (''flat shape'') between the first peak position and the second one was also reproduced by the FPMD simulation. It is known that the error bars of the evaluated $g(r)$ are quite small in the FPMD and the data scattering of $S(Q)$ is a little larger, for example, ± 0.1. Even under this condition, the particular feature of $S(Q)$ described above can be thought to be reproduced by the FPMD. These indicate the reliability of the FPMD simulation.

Because the reliability of structural information from the FPMD simulation was confirmed, it is very interesting to obtain the microscopic structure information in detail from this FPMD simulation. An angle distribution function, $g^{(3)}(\theta,r_c)$, as one type of three body distribution function, was calculated from the atomic configuration obtained by the FPMD simulation. The $g^{(3)}(\theta,r_c)$ for liquid Sn at 773 and 1873 K are shown in Fig. 8. The angle noted here was formed by a pair of vectors drawn from a reference atom to any other two atoms within a sphere of cutoff radius r_c. The $g^{(3)}(\theta,r_c)$ shows a clear peak centered at 60° in addition to the peak around 100°, when the cutoff radius, r_c, is taken to be 0.34 nm, which is far larger than the first nearest neighbor distance, 0.307–0.317 nm (see Table II). With decreasing the cutoff radius r_c, a peak around 60° seems to disappear and the $g^{(3)}(\theta,r_c)$ shows only single broad peak around 100°. It can be seen that the height of these peaks becomes lower with the increase of the temperature. However, in the case of $r_c=0.30$ nm, the height of a single broad peak does not change with the variation of the temperature. In Fig. 9, the $g^{(3)}(\theta,r_c)$ is also shown for liquid Pb, which is a typical simple ''category I'' liquid metal. As can be seen in Fig. 9, two peaks around 60° and 120°, respectively, are present irrespective of the cutoff radius r_c. The peak at 60° remains present even at higher temperatures though the lowering and the shift to high angle side can be seen.

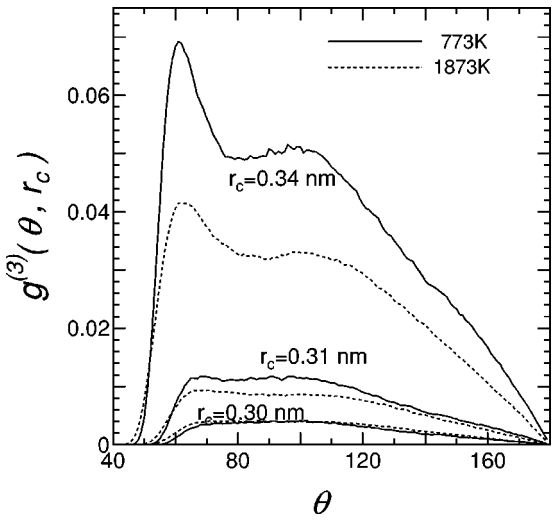

FIG. 8. The angle, θ, dependence of angle distribution function, $g^{(3)}(\theta,r_c)$, of liquid Sn in spheres with cutoff radii r_c's.

When the interatomic interaction is isotropic and the atoms are packed in a closed-packed form, the $g^{(3)}(\theta,r_c)$ should show peaks around 60° and 120°. On the other hand, in the covalent bond crystal of diamond type with anisotropic interactions, it should show the tetrahedral bond angle of 109°. Therefore, peaks around 60° and 120° of $g^{(3)}(\theta,r_c)$ in Fig. 9 correspond to the fact that the structure of liquid Pb is essentially hard sphere like or belongs to ''category I'' though some shift of the peak from 60° can be observed with the increase of the temperature and with the decrease of the cutoff radius r_c. The structure of liquid Sn seems to be more complex from the behavior of $g^{(3)}(\theta,r_c)$. The clear peak around 60° in the case of larger r_c (Fig. 8) indicates a feature of the typical simple liquid structure if we observe liquid Sn in a large scale. On the other hand, if we observe it in a smaller scale, the structure of liquid Sn seems

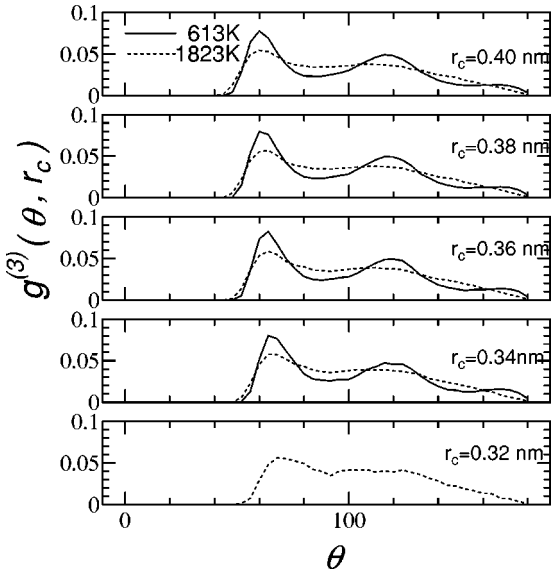

FIG. 9. The angle, θ, dependence of angle distribution function, $g^{(3)}(\theta,r_c)$, of liquid Pb in spheres with cutoff radii r_c's.

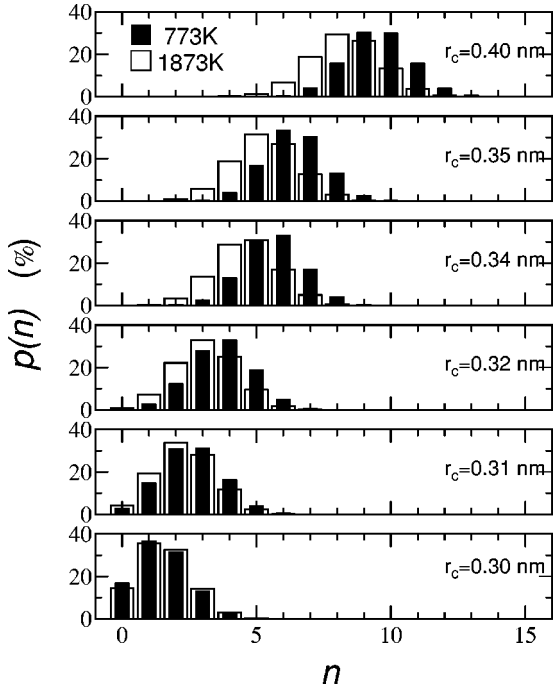

FIG. 10. The coordination number, *n*, dependence of the distribution of coordination number, $p(n)$, for liquid Sn.

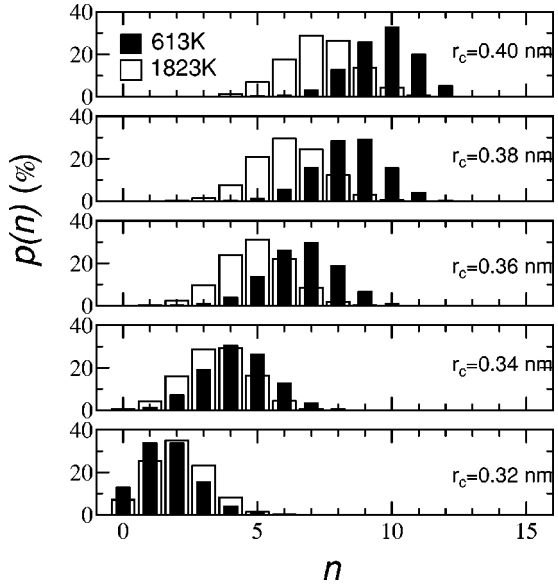

FIG. 11. The coordination number, *n*, dependence of the distribution of coordination number, $p(n)$, for liquid Pb.

to be characterized by a broad peak of $g^{(3)}(\theta,r_c)$ around 100°, which may be related to complex local structures due to anisotropic interactions or tetrahedral bond unit. In addition, on increasing temperature, the $g^{(3)}(\theta,r_c)$ for $r_c=0.30$ nm is almost unchanged. This means that the short-range structure within 0.3 nm does not so much depend on the temperature in the temperature range studied here.

From the FPMD simulation the distribution of coordination number, $p(n)$, with a given cutoff radius r_c, can be evaluated. The $p(n)$ was calculated from the number of atoms present in a sphere (''coordination number'') whose center is situated by one atom and whose radius is r_c. Figure 10 indicates the results of the relation between $p(n)$ and the coordination number, *n*, for liquid Sn both at 773 and 1873 K. The coordination number decreases with the decrease of r_c. When r_c is fixed, the coordination number decreases with the increase of temperature for $r_c \geqslant 0.32$ nm. For $r_c=0.30$ nm, however, $p(n)$ is almost unchanged with the variation of temperature. This temperature independence of $p(n)$ at smaller r_c cannot be observed for liquid Pb though the similar behavior of $p(n)$ to the case of liquid Sn can be seen for larger r_c, as shown in Fig. 11.

The difference of the temperature dependence of $g^{(3)}(\theta,r_c)$ and $p(n)$ for small r_c between liquid Sn and liquid Pb may be related to that of the microscopic liquid structure or short range structure of liquids between them. As already described, the structure of liquid Pb is rather simple and well reproduced by the hard sphere model. On the other hand, liquid Sn possesses the tendency of the formation of covalent bonds. The solid Sn just below the melting temperature forms a white tin structure (β-form), which can be considered to be a distorted diamond structure. The Sn changes from β-form to α-form (or gray Sn) of the diamond structure below 286 K. The coordination number on the most nearest neighbor site is four in these solid states. Therefore, from the structure in the solid state and from the angle distribution function shown in Fig. 8, the existence of the tetrahedral structure may be implied. Nevertheless, in the $p(n)$ of liquid Sn for $r_c=0.30$ nm (Fig. 10), the popular coordination number is 2–3. There are only a few possibilities for taking 4 as the coordination number. It can be concluded that there are no complete tetrahedral structure units but their fragments persist in the liquid state of Sn on melting. In addition, such short-range structures in liquid Sn do not change with the variation of temperature even at a high temperature of 1873 K, judging from the temperature independence of $p(n)$ for $r_c=0.3$ nm. The above described discussions are based on the average of ''snap shot'' of atomic configuration and it should be noted that the creation and the annihilation of these fragments are rapid.

Here we can also discuss the structure of liquid Sn in the common tendency among group IVB(14) liquids. It is well known that $S(Q)$'s of liquid Si and Ge also have the shoulder in the high-Q side of the first peak.[13] At the same time, their $g^{(3)}(\theta,r_c)$'s show a peak around 100°.[41,50,56–58] On the other hand, in the case of liquid Pb, which is also the group IVB(14) element without shoulder in $S(Q)$,[13] the $g^{(3)}(\theta,r_c)$ does not show the peak relating to the tetrahedral angle around 109°, as already described. These facts imply that the shoulder in $S(Q)$ of liquid Sn is related to the short-range structure making the peak around 100° in $g^{(3)}(\theta,r_c)$.

As for the origin of the shoulder in $S(Q)$, two possibilities have been considered. The double hard sphere model[18–23] provided one possibility. In this model, the domain of tetrahedral unit with some large scale was considered for liquid metals with shoulders. Here we note the fact that the structure factor of the hard sphere mixtures,[59] which corresponds to a homogeneous model of liquids, does not reproduce such shoulders under any conditions. Probably

more rigorous evidence should be given for the existence of an inhomogeneity in such liquids. In another approach, the origin of shoulders has been attributed to the form of the interionic potential.[25,26,31–33] Silbert and Young[25] showed that the shoulder in $S(Q)$ can be reproduced by an interionic potential with a ledge in the repulsive part of the interionic potential. Grimson and Silbert[26] succeeded in reproducing the shoulders in $S(Q)$ of liquid Sn by optimizing the form of the repulsive part of the interionic potential, which was added as a perturbation to the hard sphere potential, as already described in Sec. II Hafner and Kahl[31] showed that the shoulder in $S(Q)$ can be reproduced by the crossover effect between two characteristic lengths, the core radius of the Ashcroft type pseudopotential of ions and the wavelength of the Friedel oscillation; this crossover causes the ledge in the repulsive part of the interionic potential. On the other hand, Mon *et al.*[33] noted the importance of dynamically screened fluctuating dipole interaction between ion cores or the van der Waals interaction. They showed that the ledge type effective interionic potential can be derived from such core polarization effects and succeeded in reproducing the shoulder in $S(Q)$ of liquid Ga by the combination of this interionic potential with the Monte Carlo simulation of liquids. Ashcroft[34] inferred the possibility that the origin of the shoulder in liquid Si and Ge may be related to this core polarization effect. A similar approach has been quite recently performed by González *et al.*[35] for liquid Ga. Unfortunately from these studies, it still has not been clarified whether the tetrahedral unit is present in liquid metals with shoulders in $S(Q)$ or not. In the present study, we showed that at least the fragments of tetrahedral unit may be present in liquid Sn even at 1867 K. This may relate to the fact that, if the clustering of atoms may relate to the electronic effect in terms of interionic interaction, the Fermi energy of liquid Sn on the free electron model is calculated to be above 100 000 K.

The FPMD in the present theoretical analysis does not depend on the assumption of the pairwise interaction and includes the nonlinear effects on the response of electron gas and the many body force acting on one atom as the contribution of forces derived from all other atoms. The many body interaction is important for the structure and the physicochemical properties of liquids with fragments of the tetrahedral units.

C. Atomic motions in liquid Sn

From the present FPMD simulations, the information of microscopic atomic motion can be obtained. The mean square displacement (MSD) of atoms is shown in Fig. 12. Three regions can be seen in Fig. 12, the free particle behavior of parabolic time dependence (up to 0.1–0.2 ps), the region of linear time dependence of the diffusion law(from 0.3 to 0.6 ps) and the transition region between them ((0.1–0.2 ps) to (0.3–0.6 ps)). Figure 13 shows the normalized form of the velocity autocorrelation function (VAF), $Z(t)$. The normalized VAF, $Z(t)/Z(0)$, decreases rapidly with the progress of time and then the oscillatory negative regions can be seen below 1273 K. However, above 1473 K, the normalized VAF indicates no negative regions though oscillatory behaviors themselves can be seen. These indicate that the backscattering effect or cage effect is present clearly at lower temperatures. However, at high temperatures, such an effect is weaker or absent though the interaction with surrounding atoms itself still works judging from the existence of oscillatory behavior. Quite recently, Hoshino *et al.*[60] presented the detailed analysis of VAF among liquid Sn, Ge, and Na. The mode-coupling analysis is not valid for liquid Sn and Ge in addition to liquid Na at high temperatures. In Fig. 14, the power spectrum of the VAF, $Z(\omega)$, is shown. It can be seen that, in addition to the self-diffusion contribution around $\omega = 0\ \mathrm{ps}^{-1}$, broad shoulders are present around $\omega = 10$–$20\ \mathrm{ps}^{-1}$. This may relate to the existence of the longitudinal acoustic modes in liquid Sn, as was discussed for the case of liquid Ge.[50]

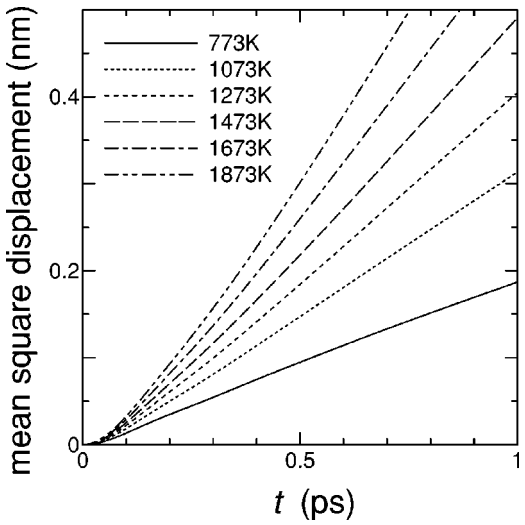

FIG. 12. The variation of the mean square displacement (MSD) with time, t, for liquid Sn.

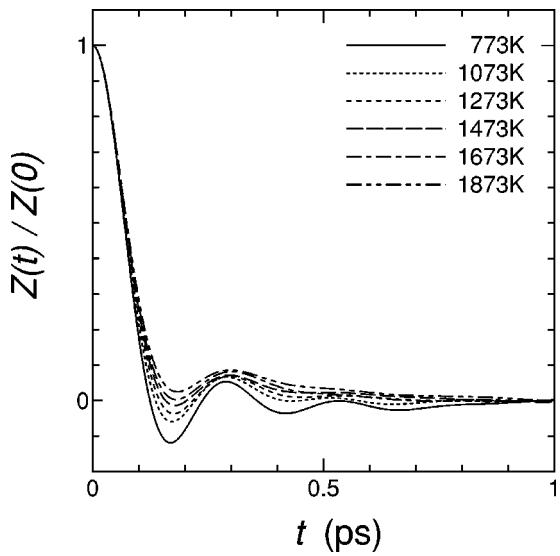

FIG. 13. The variation of the normalized velocity autocorrelation function, $Z(t)/Z(0)$, with time, t, for liquid Sn.

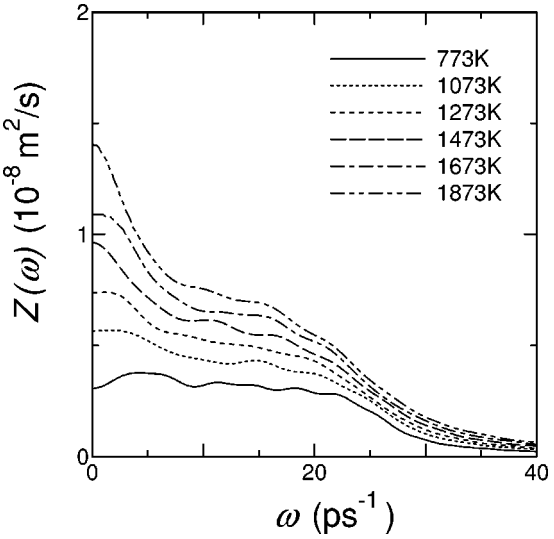

FIG. 14. The power spectrum of the velocity autocorrelation function, $Z(\omega)$, of liquid Sn.

Finally, the self-diffusion coefficient, D, is discussed. The self-diffusion coefficients, D's, are calculated both from the MSD of atoms and from the VAF. Since the simulations were carried out for long time, 36–48 ps (10 000 step), the results obtained from the MSD and the VAF are in good agreement with each other. The D values of our present simulation, shown in Fig. 15, are about half of the experimental D obtained under microgravity,[10–12] in spite of the fact that the calculated structure factors, $S(Q)$'s, of liquid Sn are in excellent agreement with the experimental $S(Q)$'s. In addition, it is far smaller than the D due to the long capillary method on the ground by Ma and Swalin[61] and smaller than that due to the shear cell technique by Bruson and Gerl.[62] At present

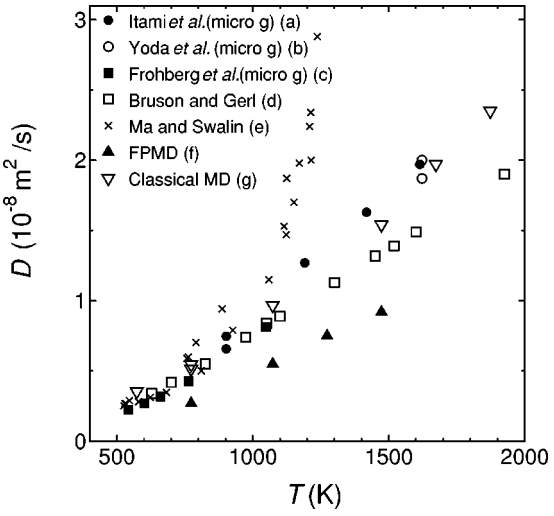

FIG. 15. The self-diffusion coefficient, D, of liquid Sn as a function of temperature, T; microgravity experiments: (a) Itami *et al.*, (Ref. 11), (b) Yoda *et al.* (Ref. 12), and (c) Frohberg *et al.* (Refs. 9 and 10); experiments on the ground: (d) Bruson and Gerl (Ref. 62) and (e) Ma and Swallin (Ref. 61); molecular dynamics (MD): (f) the present first-principle MD (FPMD), and (g) the present classical MD.

it might be concluded that, among self-diffusion experiments for liquid Sn, the smallest D was found to be given by Bruson and Gerl.[62] However it is the fact that the shear cell technique has a tendency for giving lower values of D if errors, such as a misalignment of joining into liquid diffusion columns, are mixed in the experimental data; in addition, there is a tendency that the long capillary method suffers easily from the convection on the ground and the segregation.[5,9] On the other hand, the independent measurements under microgravity[10–12] provided a single temperature dependence of D for liquid Sn irrespective of data sources and they may be considered to be reliable, as was discussed elsewhere.[63] Needless to say, further accurate experiments, probably in the ISS, must be performed for obtaining the final answer about the question what is the true self-diffusion coefficient for liquid Sn.

One of problems in the present simulation is the small system size in the FPMD simulation. To check the size dependence of D, we have performed the FPMD simulation for liquid Sn at 773 K using a larger system composed of 125 atoms for 800 time steps. Though the statistical average for D in this short time simulation is not so good, the result of D is about 30% larger than that calculated in the system of 64 atoms with the same time steps. One of the other factors for the improvement of the calculated value of D may be the pressure of the system in the simulation. In our MD simulation the experimental value of the density[52] was used at each temperature. When the density and the temperature are fixed, the pressure is uniquely determined in the thermodynamics. However, since our simulation was carried out under constant number of atoms, constant temperature, and constant volume (NVT ensemble) in the small systems, the pressure may not be the same as the macroscopic one. To examine the size dependence of the self-diffusion coefficient for liquid Sn using a larger system, classical MD simulations were performed with the number of atoms from 64 to 2197. For this classical simulation, the temperature dependence of the interionic potential was obtained from the inverse problem method,[64,65] namely it was determined to reproduce the temperature dependence of experimental $S(Q)$ obtained in the present study. On this procedure, the value of $S(Q)$ in the low Q region was important and the present $S(Q)$'s in this low Q region were slightly larger, as already described. To improve the accuracy of this method, the $S(Q)$ in the low Q region was obtained by the small angle x-ray structure analysis of liquid Sn; its details was described elsewhere.[66] It was found that the calculated values of D are almost unchanged if more than 1000 atoms are used and they depend on the system size, when the number of atoms is less than 500. The value of D obtained by this classical MD with 2197 atoms is about 20% larger than that obtained by the FPMD with 64 atoms. As can be seen in Fig. 15, rather good agreement of D was obtained between this classical MD simulation and the microgravity experiment. This considerable agreement of D is derived from the incorporation of particular feature of liquid structures, shoulders or the fragment of tetrahedral units, in terms of the experimental structure factor. The explicit role of many body interaction on the mechanism of atomic motion may be a future problem. Quite recently, the similar

good agreement of D for liquid Sn was obtained between the classical MD and the microgravity diffusion data by Belashchenko,[67] though the employed interionic potential by him was obtained rather by a simplified inverse method. He obtained interionic potentials by inserting experimental $S(Q)$'s into an approximate theory of liquids, the mean potential approximation.[68] The inverse method in the present study, employed for the evaluation of the interionic potential of liquid Sn, is based on the exact theory of liquids within the pair potential approximation, that is the exact cluster (density) expansion of the $g(r)$.[69,70]

V. SUMMARY

In this study, the neutron scattering experiments and the FPMD simulations were performed for liquid Sn. From the neutron scattering experiments, a shoulder on the high-Q side of the first peak of $S(Q)$ can be clearly seen at 573 and 773 K. Even at 1873 K, such a shoulder may be present though it becomes unclear in the change of overall pattern of $S(Q)$. From the FPMD simulations, a broad peak around 100° on the angle distribution function is observed up to 1873 K. The coordination number, n, with cutoff radius of 0.30 nm does not change with the increase of temperature from 773 to 1873 K though it decreases with the increase of temperature for larger cutoff radius. These features were not found by the FPMD simulation for liquid Pb, which is a typical closely packed liquid metal. Therefore, these features for liquid Sn indicate that at least the fragments of tetrahedral unit may persist even at high temperatures in liquid Sn. As for the self-diffusion coefficient, D, the classical molecular-dynamics simulation with a large number of atoms was employed. The interionic potential was determined by the inverse method, in which the present $S(Q)$'s were employed together with the $S(Q)$'s in the low Q region due to the small angle x-ray scattering. Obtained D's are in good agreement with experimental values under microgravity.

*Invited Researcher in National Space Development Agency of Japan (NASDA), 2-1-1 Sengen, Tsukuba 305-8505, Japan. Electronic mail address: itami.toshio@nasda.go.jp

†Present address: Hijiyama University, Hiroshima, 732-8509, Japan.

‡Present address: Kanazawa University, Kanazawa, 920-1192, Japan.

§Present address: Kumamoto University, Kumamoto, 860-8555, Japan.

[1] J. M. Ziman, Philos. Mag. **6**, 1013 (1961).

[2] N. W. Ashcroft and D. Stroud, *Solid State Physics* (Academic, New York, 1978), Vol. 33, p. 1.

[3] A. Rice and P. Gray, *The Statistical Mechanics of Simple Liquids* (Interscience, New York, 1965).

[4] J. P. Hansen and I. R. McDonald, *Theory of Simple Liquids* (Academic, London, 1976).

[5] M. Shimoji and T. Itami, *Atomic Transport in Liquid Metals* (Trans Tech, Switzerland, 1986); see also M. Shimoji, *Liquid Metals* (Academic, London, 1977).

[6] U. Balucani and M. Zoppi, *Dynamics of the Liquid State* (Clarendon, Oxford, 1994).

[7] S. Chapman and T. G. Cowling, *The Mathematical Theory of Non-Uniform Gases* (Cambridge University Press, London, 1939).

[8] B. J. Alder and T. E. Wainwright, Phys. Rev. Lett. **18**, 988 (1967); J. Chem. Phys. **53**, 3813 (1970).

[9] G. Frohberg, *Material Sciences in Space* (Springer, Berlin, 1986), p. 425; see also Y. Malmejac and G. Frohberg, *Fluid Sciences and Materials Science in Space* (Springer, Berlin, 1987), p. 159.

[10] G. Frohberg, K. H. Kraatz, and H. Weber, in *Proceedings of the Sixth European Symposium on Material Sciences Under Microgravity Conditions*, Bordeaux, 1986.

[11] T. Itami, H. Aoki, M. Kaneko, M. Uchida, A. Shisa, S. Amano, O. Odawara, T. Masaki, H. Oda, T. Ooida, and S. Yoda, J. Jpn. Soc. Microgravity Appl. **15**, 225 (1998); T. Itami *et al.*, Microgravity Science Laboratory(MSL-1) Final Report (NASA/CP-1998-208868, compiled by M. B. Robinson, 1998), p. 59.

[12] S. Yoda, T. Masaki, and H. Oda, J. Jpn. Soc. Microgravity Appl. Suppl. II **15**, 343 (1998); S. Yoda *et al.*, Microgravity Science Laboratory (MSL-1) Final Report (NASA/CP-1998-208868, compiled by M. B. Robinson, 1998), p. 86.

[13] Y. Waseda, *The Structure of Non-Crystalline Materials, Liquid and Amorphous Solid* (McGraw-Hill, New York, 1980).

[14] S. Takeda, S. Tamaki, and Y. Waseda, J. Phys. Soc. Jpn. **53**, 3447 (1984).

[15] A. G. Wells, *Structural Inorganic Chemistry*, 4th ed. (Clarendon, Oxford, 1975).

[16] L. I. Berger, *Semiconductor Materials* (CRC Press, Boca Raton, FL, 1996).

[17] N. W. Ashcroft and J. Leckner, Phys. Rev. **145**, 83 (1966).

[18] B. R. Orton, Z. Naturforsch. **34A**, 1547 (1979).

[19] B. R. Orton, Z. Naturforsch. A **30**, 1500 (1975).

[20] B. R. Orton, Z. Naturforsch. A **31**, 397 (1976).

[21] B. R. Orton, Z. Naturforsch. A **32**, 332 (1977).

[22] B. R. Orton, J. Phys. (Paris) **41**, C8 (1980).

[23] J. P. Gabather and S. Steeb, Z. Naturforsch. A **34A**, 1314 (1979).

[24] V. Petkov and G. Yunchov, J. Phys.: Condens. Matter **6**, 10 885 (1994).

[25] M. Silbert and W. H. Young, Phys. Lett. **58A**, 469 (1976).

[26] M. J. Grimson and M. Silbert, J. Phys. F: Met. Phys. **14**, L95 (1984).

[27] V. Heine and D. Weaire, *Solid State Physics*, Vol. 24 (Academic, New York, 1970), p. 250.

[28] J. Hafner and V. Heine, J. Phys. F: Met. Phys. **13**, 2475 (1983).

[29] I. Yokoyama and S. Ono, J. Phys. F: Met. Phys. **15**, 1215 (1985).

[30] K. Hoshino, C. H. Leung, L. McLaughlin, S. R. M. Rahman, and W. H. Young, J. Phys. F: Met. Phys. **18**, 787 (1987).

[31] J. Hafner and G. Kahl, J. Phys. F: Met. Phys. **14**, 2259 (1984).

[32] W. Jank and J. Hafner, Phys. Rev. B **41**, 1497 (1990).

[33] K. K. Mon, N. W. Ashcroft, and G. V. Chester, Phys. Rev. B **19**, 5103 (1979).

[34] K. K. Mon, N. W. Ashcroft, and G. V. Chester, Nuovo Cimento **12**, 597 (1990).

[35] L. E. González, D. J. González, and M. Silbert, Mol. Phys. **99**, 875 (1999).

[36] F. H. Stillinger and T. A. Weber, Phys. Rev. B **31**, 5262 (1985).

[37] J. Tersoff, Phys. Rev. B **38**, 9902 (1988); **39**, 5566 (1989).
[38] N. Takeuchi and I. L. Garzón, Phys. Rev. B **50**, 8342 (1994).
[39] M. Ishimaru, K. Yoshida, and T. Motooka, Phys. Rev. B **53**, 7176 (1996).
[40] M. Ishimaru, K. Yoshida, T. Kumamoto, and T. Motooka, Phys. Rev. B **54**, 4638 (1996).
[41] I. Štich, R. Car, and M. Parrinello, Phys. Rev. B **44**, 4262 (1991).
[42] R. Car and M. Parrinello, Phys. Rev. Lett. **55**, 2471 (1985).
[43] S. Munejiri, T. Masaki, Y. Ishii, T. Kamiyama, Y. Senda, F. Shimojo, K. Hoshino, and T. Itami, J. Phys. Soc. Jpn. Suppl. A **70**, 268 (2001).
[44] H. H. Paalman and C. J. Pings, J. Appl. Phys. **33**, 2635 (1962).
[45] I. A. Blech and B. L. Averbach, Phys. Rev. **137**, 1113 (1965).
[46] J. L. Yarnell, M. J. Katz, R. G. Wenzel, and S. H. Koenig, Phys. Rev. A **7**, 2130 (1973).
[47] D. M. Ceperley and B. J. Alder, Phys. Rev. Lett. **45**, 566 (1980); J. P. Perdew and A. Zunger, Phys. Rev. B **23**, 5048 (1981).
[48] N. Troullier and L. L. Martines, Phys. Rev. B **43**, 1993 (1991).
[49] M. P. Teter, M. C. Payne, and D. C. Allan, Phys. Rev. B **40**, 12 255 (1989).
[50] G. Kresse and J. Hafner, Phys. Rev. B **49**, 14 251 (1994).
[51] F. Shimojo, Y. Zempo, K. Hoshino, and M. Watabe, Phys. Rev. B **52**, 9320 (1995).
[52] P. M. Nasch and S. G. Steinemann, Phys. Chem. Liq. **29**, 43 (1995).
[53] S. Nosé, Mol. Phys. **52**, 255 (1984).
[54] W. G. Hoover, Phys. Rev. A **31**, 1695 (1985).
[55] L. D. Lucas, *Techniques del Ingĕnieur* (Paris, 1984), Vol. 7, pp. M65–1.
[56] I. Štich, R. Car, and M. Parrinello, Phys. Rev. Lett. **63**, 2240 (1989).
[57] C. Z. Wang, C. T. Chan, and K. M. Ho, Phys. Rev. B **45**, 12 227 (1992).
[58] R. V. Kulkarni, W. G. Aulbur, and D. Stroud, Phys. Rev. B **55**, 6896 (1997).
[59] N. W. Ashcroft and D. C. Langreth, Phys. Rev. **156**, 685 (1967).
[60] K. Hoshino, F. Shimojo, and S. Munejiri, J. Phys. Soc. Jpn. **71**, 119 (2002).
[61] C. H. Ma and R. A. Swallin, J. Chem. Phys. **46**, 3014 (1962).
[62] A. Bruson and M. Gerl, Phys. Rev. B **21**, 5447 (1980).
[63] T. Itami, T. Masaki, H. Aoki, S. Munejiri, M. Uchida, S. Matsumoto, T. Kamiyama, and K. Hoshino, J. Non-Cryst. Solids **312-314**, 177 (2002).
[64] L. Reatto, D. L. Levesque, and J. J. Weis, Phys. Rev. A **33**, 3451 (1986).
[65] S. Munejiri, F. Shimojo, K. Hoshino, and M. Watabe, J. Phys. Soc. Jpn. **64**, 344 (1995).
[66] T. Masaki, H. Aoki, S. Munejiri, Y. Ishii, and T. Itami, J. Non-Cryst. Solids **312-314**, 191 (2002).
[67] D. K. Belashchenko, J. Phys. Chem. **75**, 81 (2001).
[68] N. E. Cusack, *The Physics of Structurally Disordered Matter* (IOP, Bristol, 1987).
[69] J. E. Mayer and E. Montroll, J. Chem. Phys. **9**, 2 (1941); E. E. Salpeter, Ann. Phys. (N.Y.) **5**, 183 (1958).
[70] T. Itami, *Condensed Matter-Disordered Solids* (World Scientific, Singapore, 1995), p. 123.